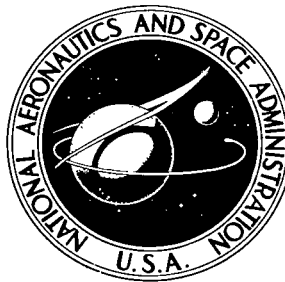


NASA TECHNICAL NOTE



NASA TN D-5533

c. 1

NASA TN D-5533



LOAN COPY: RETURN TO
AFWL (WL0L)
KIRTLAND AFB, N MEX

WAVELENGTH DEPENDENCE OF LASER BEAM SCINTILLATION

by M. W. Fitzmaurice, J. L. Bufton, and P. O. Minott

*Goddard Space Flight Center
Greenbelt, Md.*

NATIONAL AERONAUTICS AND SPACE ADMINISTRATION • WASHINGTON, D. C. • DECEMBER 1969



WAVELENGTH DEPENDENCE OF
LASER BEAM SCINTILLATION

By M. W. Fitzmaurice, J. L. Bufton, and P. O. Minott

Goddard Space Flight Center
Greenbelt, Md.

NATIONAL AERONAUTICS AND SPACE ADMINISTRATION

For sale by the Clearinghouse for Federal Scientific and Technical Information
Springfield, Virginia 22151 - Price \$3.00

ABSTRACT

An experiment was performed to confirm the proportionality of log-amplitude variance and the $7/6$ power of wave number predicted by Tatarski for horizontal propagation from a spherical-wave transmitter to a point detector. The validity of this proportionality was tested for two wavelengths, 0.632 and 10.6 microns. A 0.632μ He-Ne laser and a 10.6μ CO₂ laser transmitter were operated simultaneously over a folded 1.1-km horizontal path, and the beams were detected by a photomultiplier and a gold-doped germanium detector. The primary scintillation statistic, log-amplitude variance, was evaluated for each wavelength on a digital computer. The ratio of variances at 0.632 and 10.6 microns was in close agreement with predictions. Power spectral density, autocorrelation, and cumulative probability density also were evaluated for each wavelength. Scintillation statistics at 10.6μ were found to be log-normal, just as in the visible portion of the spectrum.

CONTENTS

Abstract	ii
INTRODUCTION	1
EXPERIMENTAL TECHNIQUE	1
RESULTS	2
CONCLUSIONS	8
ACKNOWLEDGMENTS	8
References	8

WAVELENGTH DEPENDENCE OF LASER BEAM SCINTILLATION*

by

M. W. Fitzmaurice, J. L. Bufton, and P. O. Minott
Goddard Space Flight Center

INTRODUCTION

Theoretical analyses by several investigators have led to predictions that the strength of optical scintillation depends strongly on wavelength. Recent statistical studies are couched in terms of log amplitude, $\ell(t)$, defined as

$$\ell(t) = 1/2 \log_{\ell} I(t)/I_0 \quad , \quad (1)$$

where $I(t)$ is the instantaneous irradiance, and I_0 is the mean irradiance. Using the Kolmogoroff model of turbulence, it can be shown (References 1 and 2) that, for horizontal paths, the variance of $\ell(t)$ (σ_{ℓ}^2) is

$$\sigma_{\ell}^2 \approx k^{7/6} z^{11/6} C_N^2 \quad , \quad (2)$$

where

$$\begin{aligned} k &= \text{wave number,} \\ z &= \text{range,} \\ C_N^2 &= \text{refractive index structure constant.} \end{aligned}$$

We have conducted an experiment to test the validity of the wavelength dependence predicted by this expression.

EXPERIMENTAL TECHNIQUE

Because of the short-term stationarity and the lack of statistical homogeneity of the atmosphere, the experimenter must transmit simultaneously through the same portion of the atmosphere at each wavelength of interest. The experiment for this report is shown schematically in Figure 1. A He-Ne laser at 0.632 micron and a CO₂ laser at 10.6 microns were aligned parallel, with an offset of 12 cm; and were operated over a folded horizontal 1.2-km path. The He-Ne output was unmodulated and no external optics were used, so that the assumptions of a spherical wave transmitter were satisfied. The CO₂ output

*Presented to the Spring 1968 Meeting of the Optical Society of America, Washington, D.C.

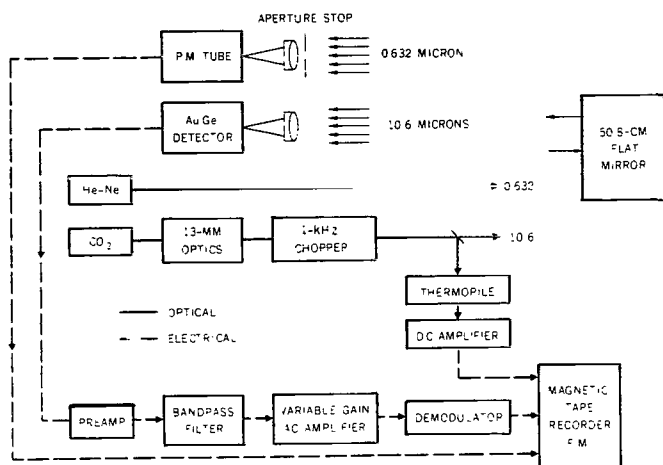


Figure 1—Experiment schematic diagram.

was modulated at a 1-kHz rate to minimize the background and to enhance the detector operation. The 10.6-micron beam was transmitted through a 13-mm-aperture telescope which, because of the longer wavelength, also approximated a spherical wave source. A small portion of the CO₂ beam was diverted and detected by a thermopile to monitor any fluctuations in output power.

A mirror in the field reflected the two beams, and they were then detected at the transmitter station by a photomultiplier and a gold-doped germanium detector. The output of the photomultiplier tube was recorded directly on an FM tape recorder. The 10.6-micron detected signal was demodulated by means of a standard envelope detection scheme and then recorded.

Table 1 lists the important parameters of the experiment. In order to avoid the effects of aperture-averaging, each detector aperture was made to approximate a point detector. In addition, the photomultiplier tube aperture was adjusted so as to make the ratio of the apertures equal to the square root of the ratio of the wavelengths. This ensured that aperture-averaging effects were insignificant.

The recorded scintillation data were replayed through an A/D converter into a Raytheon 520 digital computer that analyzed the statistics of the scintillation. The computer was programmed to analyze both irradiance and log-amplitude statistics. Available statistics and functional relationships are given in Table 2. The analog scintillation signal was sampled at a 1-kHz rate for 10 seconds, with each sample assigned to one of 500 discrete levels available in the computer. The selection of the time-record length for a single data run is a tradeoff between the statistical reliability of a measurement and the statistically time-varying atmosphere. After the bandwidth of the scintillation was evaluated, a 10-second record appeared to be a near-optimum choice.

RESULTS

Figure 2 shows the results of measurements taken over a 2-hour nighttime period in December. Plotted along the Y-axis is the parameter ψ defined as the ratio of log-amplitude variances at 0.632 and 10.6 microns. The X-axis is the log-amplitude variance for the He-Ne beam and the refractive index structure constant C_N^2 , which in this case

Table 1

Experimental Parameters

Parameter	CO ₂	He-Ne
Output power	2 watts	1 mw
Beam divergence	0.4 mr	0.7 mr
Beam diameter	13 mm	1.4 mm
Detector aperture	2.5 cm	.62 cm
Detector field of view	2	5
Detection signal bandwidth	220 Hz	2.5 kHz
Chopper frequency	1 kHz	
Range	1.2 km	1.2 km
Average beam height	4m	4m
Folding mirror diameter	50.8 cm	50.8 cm
Length of data run	10 sec	10 sec

was determined from the equations for horizontal spherical wave propagation. The value 26.7 is the theoretical ratio obtained from the 7/6 power predictions.

The data would seem to indicate that the scintillation statistics depart from the 7/6 power law in the region to the left. The difficulty here is that region to the left corresponds to very low turbulence. The CO₂ laser output unfortunately had an appreciable amount of 120-Hz power supply ripple. In this region, the dominant noise on the 10.6-micron signal was caused not by the atmosphere but by the 120-Hz ripple. The output of the CO₂ unit was recorded on tape; and an evaluation of the magnitude of the ripple showed that, in the 0.04 region, the internal laser modulation became the same order of magnitude as the atmospheric-induced modulation. Therefore, the data points in the region below 0.07 are of questionable value. Some compensation for the CO₂ internal noise can be accomplished if one makes appropriate assumptions.

The intensity at the detector aperture can be considered (Reference 3) as the product of two random variables,

$$I(t) = I_L h(t) \quad (3)$$

The first, I_L , is the irradiance fluctuation caused by internal laser ripple; the second, $h(t)$, is the time-varying atmospheric transmission. If both variables are assumed log-normal with respective variances σ_1^2 and σ_2^2 , their product is also log-normal with a variance equal to $\sigma_1^2 + \sigma_2^2$. Several experiments (References 3 and 4) have shown $h(t)$ to be log-normal (in the visible spectrum), and inspection of cumulative density of log amplitude for the transmitter noise (Figure 3) has indicated normality as a reasonable approximation.

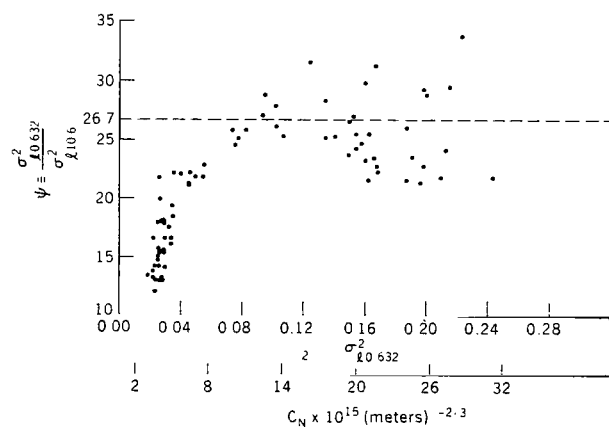


Figure 2—Ratio of log-amplitude variance for He-Ne and CO₂ wavelengths.

Table 2
Computer Analysis

Irradiance statistics	Log-amplitude statistics
Average value	Average value
Variance	Variance
Median	Median
3rd central moment	3rd central moment
4th central moment	4th central moment
Probability density function	Probability density function
	Cumulative distribution function
Power spectral density	
Autocorrelation function	

The data are shown replotted in Figure 4 with the transmitter noise subtracted from the CO₂ statistics; the measurements obtained during low-scintillation conditions are neglected. The average value of the 39 independent data points shown is 26.8, and their variance is 10.8. The average value of ψ is in close agreement with the predicted value of 26.7.

The statistical reliability of the measurements has been analyzed to determine the magnitude of

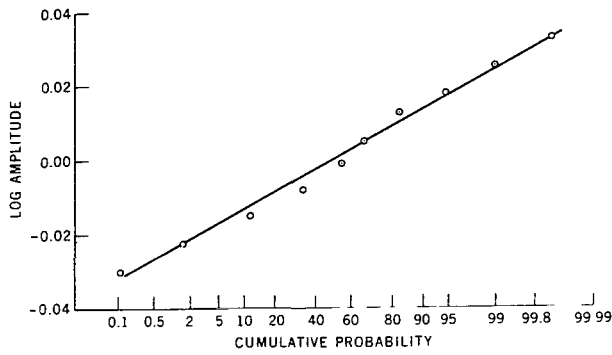


Figure 3—CO₂ transmitter noise; log amplitude-cumulative probability.

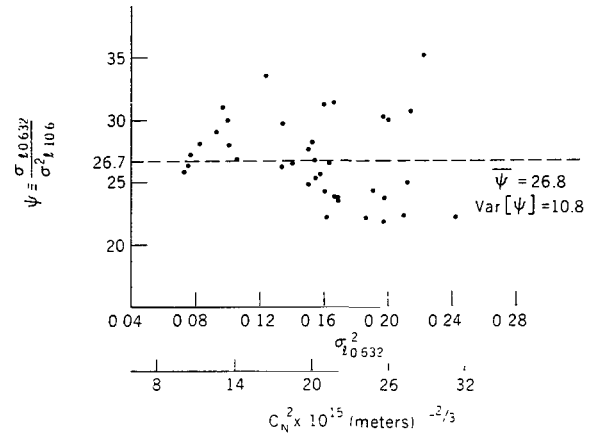


Figure 4—Ratio of log-amplitude variances for He-Ne and CO₂ wavelengths (transmitter noise removed, and all data $\sigma_{10.632}^2$ less than 0.07 neglected).

data scatter to be expected under ideal conditions. Given a random variable x (in this case, log amplitude) with probability density $f(x)$, mean μ_x , and variance σ_x^2 , we can select a random sample of size n and form the statistics \bar{X} (sample mean) and S^2 (sample variance), where*

$$\bar{X} \equiv \frac{1}{n} \sum_{i=1}^n x_i, \quad (4)$$

and

$$S^2 \equiv \frac{1}{n} \sum_{i=1}^n (x_i - \bar{X})^2. \quad (5)$$

Both of these quantities are function of random variables and therefore are random variables also. With E being the expectation operator,

$$E(\bar{X}) = \mu_x, \quad (6)$$

$$E(S^2) = \left(\frac{n-1}{n} \right) \sigma_x^2, \quad (7)$$

$$E\{[S^2 - E(S^2)]^2\} = \text{variance}(S^2) = \frac{m_4 - m_2^2}{n} - \frac{2(m_4 - 2m_2^2)}{n^2} + \frac{m_4 - 3m_2^2}{n^3} \quad (8)$$

*The statistics \bar{X} and S^2 are maximum likelihood estimators for μ_x and σ_x^2 . The amount of bias in S^2 becomes insignificant for large samples.

where n is the number of independent samples, and m_i is the i^{th} central moment. Each data run consisted of 10,000 samples from the scintillation signal; however, because of the finite bandwidth of the scintillation, the number of independent samples is much less than 10,000. The number of independent samples is (Reference 5)

$$n = 2 B_{\text{eq}} T \quad (9)$$

where B_{eq} is the equivalent white noise bandwidth of the signal, and T is the length of the time record; B_{eq} is approximated by (Reference 5)

$$B_{\text{eq}} = \frac{R_x(0)}{2 \int_{-\infty}^{\infty} R_x(\tau) d\tau} \quad (10)$$

where $R_x(\tau)$ is the autocorrelation function for the scintillation at time-lag τ .

The authors have evaluated the autocorrelation function experimentally for both wavelengths and thereby determined the equivalent bandwidth. Typically, the bandwidth of the He-Ne signal is several times that of the CO_2 ; therefore, the dispersion of the He-Ne sample variance is much less than that of the CO_2 . In a strict sense, the equivalent bandwidth referred to in Equations 9 and 10 should be the bandwidth of the log irradiance signal and not the bandwidth of the irradiance fluctuations. However, the data reduction system did not permit an evaluation of the spectrum of log irradiance; therefore, the equivalent bandwidth of the irradiance signal was used. It is easy to show that the bandwidth of the irradiance signal is not seriously affected by the logarithmic operation under weak scintillation conditions (which is the situation at 10.6 microns, for most paths). Consider a system with input $x = \nu_0 + \nu(t)$ and output $y = A \log x$,

where

$$\nu_0 = \text{constant (dc level),}$$

$$\nu(t) = \text{random time function with mean value equal to zero,}$$

and

$$A = \text{constant (gain of the log-amplifier).}$$

Power spectral density (psd) analysis of the input x is performed on $\nu(t)$ only, since ν_0 merely results in a delta function at the origin in the frequency domain. The output of the system is

$$y = A \log [\nu_0 + \nu(t)] = A \log (\nu_0) \left[1 + \frac{\nu(t)}{\nu_0} \right] = A \log (\nu_0) + A \log \left[1 + \frac{\nu(t)}{\nu_0} \right].$$

Therefore, psd analysis of the output needs to be performed only on the second term, since $A \log [\nu_0]$ is a constant. However,

$$\log(1+x) \approx x \quad \text{for } x \ll 1;$$

therefore,

$$\log \left[1 + \frac{\nu(t)}{\nu_0} \right] \approx \frac{\nu(t)}{\nu_0} \quad \text{for } \nu(t) \ll \nu_0 \text{ (i.e., weak scintillation).}$$

Thus, psd analysis of y is equivalent to psd analysis of $A \nu(t)/\nu_0$; this is the same as psd analysis of the input x since the constant factors A, ν_0 are removed by dividing through by the mean-square value.

If n is known, and typical values for the log-amplitude central moments are used, numerical manipulation shows that, for a 1-standard deviation scatter in the sample variances, the parameter ψ can be expected to fluctuate by approximately ± 1.5 . Therefore, the observed experimental scatter in ψ is of the same order of magnitude as that which can be expected statistically from the finite data samples.

The normalized power spectral density for both wavelengths for a particular data run is shown in Figure 5. These functions were evaluated by means of a Fourier transformation of their respective autocorrelation functions. Both curves are normalized by their intensity variances. Thus, if each wavelength has equal amounts of scintillation, this plot would indicate spectral distribution of the scintillation. The normalization scheme used requires the height of the CO₂ plot to be increased by a factor of 16. Therefore, it should be clear that, at any frequency, there is far more scintillation in the visible spectrum that at 10 microns. The resolution bandwidth is 5Hz, and the wind velocity perpendicular to the propagation path is approximately 3 mph. The power supply ripple on the 10-micron beam is obvious in this plot.

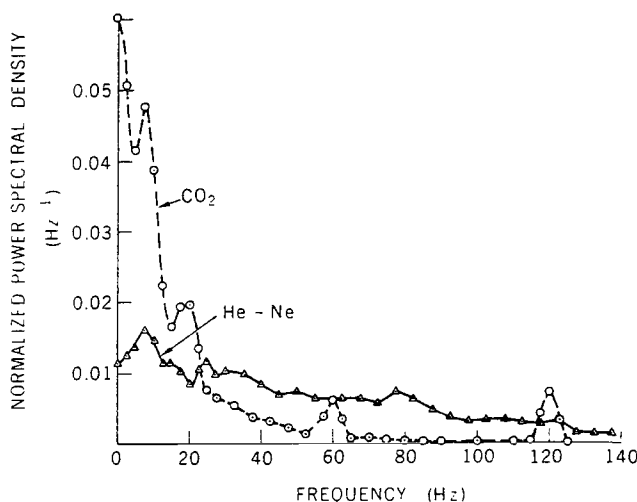


Figure 5—Dual wavelength normalized power spectral density (resolution bandwidth = 5Hz; each curve normalized to the same area; log-amplitude variances for these data are $\sigma^2_{\ell(0.632)} = 0.200$ and $\sigma^2_{\ell(10.6)} = 0.00693$).

Figure 6 presents the same data in the time domain in terms of the normalized autocorrelation function. Again, the internal modulation of the CO₂ laser appears as peaks at 8- and 16-millisecond intervals. If one fits an exponential function of the form $e^{-\alpha\tau}$ to each of these curves, the correlation time constants (the alphas) have a ratio of 4.4, which is close to the ratio of the square root of the wavelengths. An alternate interpretation is that the time required for the autocorrelation function to decrease to the $1/e$ point is proportional to the square root of wavelength. This experimental relationship has been noted in much of our data but has not been analyzed extensively.

A typical portion of the analog scintillation signal is shown in Figure 7. The computer

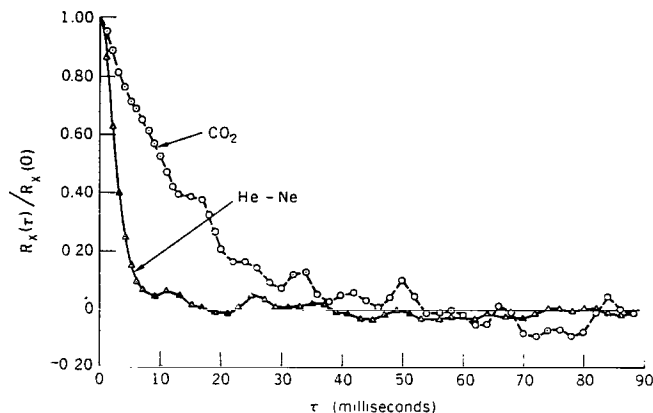


Figure 6—Normalized auto correlation function for dual wavelength scintillation; fitting the data with the exponential $e^{-\alpha\tau}$ gives $(\text{CO}_2) = 71.4$, $\alpha(\text{He-Ne}) = 312$.

evaluated the variances as 0.200 and 0.00668, which gives a ψ value of 30. The chart recorder had a 110-Hz, 3-db bandwidth, which tends to smooth some of the high-frequency He-Ne scintillation (very little CO_2 scintillation is in the 110-Hz region). The important parameter is the ratio of the maximum and minimum signal excursions from the average value. For the He-Ne scintillation, excursions of several octaves are common. In both of these traces, the background levels were not significantly different from the zero level.

Figure 8 is typical cumulative probability plot of log amplitude at 10.6 microns on Gaussian probability paper. The abscissa is $F(\ell)$, where

$$F(\ell) = \int_{-\infty}^{\ell} f(u) du, \quad (11)$$

$f(u)$ being the probability density function for log amplitude. The ordinate is log amplitude, which is defined in Equation 1. The abscissa scale is constructed so that a normal random variable would plot as a straight line. Thus it is clear that the statistics of scintillation at 10.6 microns satisfy this test for log-normality.

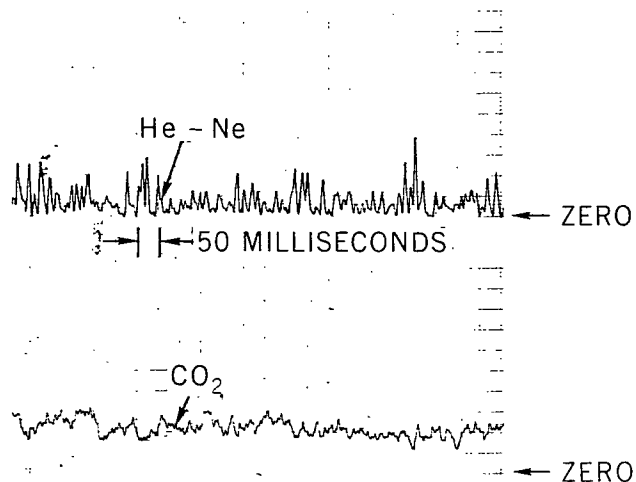


Figure 7—Typical analog scintillation signal; log-amplitude variances are 0.200 for He-Ne, and 0.00668 for CO_2 .

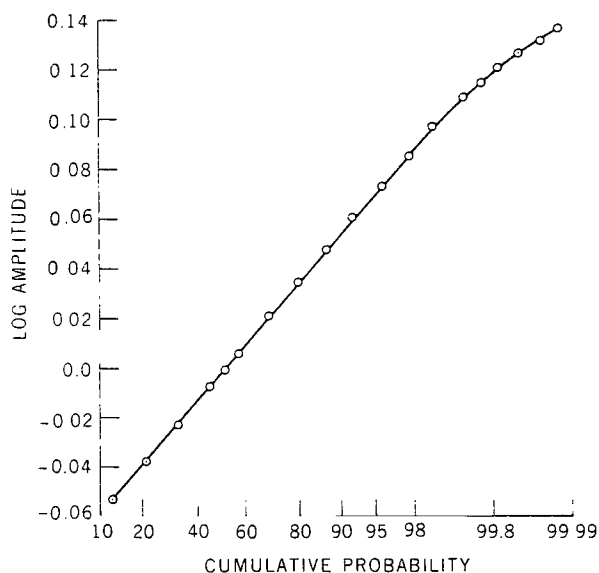


Figure 8—Cumulative probability of log amplitude at 10.6 microns; data plotted on a Gaussian abscissa scale.

CONCLUSIONS

In summary, the following conclusions can be made.

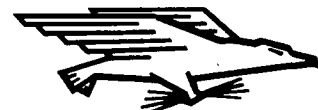
1. The average value for the log-amplitude variance ratio at 10.6 and 0.632 microns is very close to the predicted value of 26.7.
2. The CO₂ scintillation has a bandwidth that is several times less than for the He-Ne, and a correlation time that is approximately 4.5 times greater than for the He-Ne.
3. The probability distribution of scintillation at 10.6 microns is log-normal just as in the visible spectrum.

Goddard Space Flight Center
National Aeronautics and Space Administration
Greenbelt, Maryland, November 14, 1968
039-02-01-10-51

REFERENCES

1. Tatarski, V. I., "Wave Propagation in a Turbulent Medium," New York:McGraw-Hill Book Co., 1961.
2. Fried, D. L., "Propagation of a Spherical Wave in a Turbulent Medium," *J. Opt. Soc. Am.* 57:175, February 1967.
3. Gracheva, M. E., and Gurvich, A. S., "Strong Fluctuations in the Intensity of Light Propagated Through the Atmosphere Close to the Earth," *Radiofizika* 8(4):511-515, 1965.
4. Fried, D. C., Mevers, G. E., and Keister, M. P., Jr., "Measurements of Laser-Beam Scintillation in the Atmosphere," *J. Opt. Soc. Am.* 57:787, June 1967.
5. Bendat, J. S., and Piersol, A. G., "Measurement and Analysis of Random Data," New York: John Wiley and Sons, Inc., 1966.

FIRST CLASS MAIL



POSTAGE AND FEES PAID
NATIONAL AERONAUTICS AND
SPACE ADMINISTRATION

010 001 31 51 305 59345 00903
AIR FORCE RESEARCH AND DEVELOPMENT
KIRTLAND AIR FORCE BASE, NEW MEXICO 8711

RECEIVED AIR FORCE BASE, NEW MEXICO 8711

POSTMASTER: If Undeliverable (Section 158
Postal Manual) Do Not Return

"The aeronautical and space activities of the United States shall be conducted so as to contribute . . . to the expansion of human knowledge of phenomena in the atmosphere and space. The Administration shall provide for the widest practicable and appropriate dissemination of information concerning its activities and the results thereof."

— NATIONAL AERONAUTICS AND SPACE ACT OF 1958

NASA SCIENTIFIC AND TECHNICAL PUBLICATIONS

TECHNICAL REPORTS: Scientific and technical information considered important, complete, and a lasting contribution to existing knowledge.

TECHNICAL NOTES: Information less broad in scope but nevertheless of importance as a contribution to existing knowledge.

TECHNICAL MEMORANDUMS: Information receiving limited distribution because of preliminary data, security classification, or other reasons.

CONTRACTOR REPORTS: Scientific and technical information generated under a NASA contract or grant and considered an important contribution to existing knowledge.

TECHNICAL TRANSLATIONS: Information published in a foreign language considered to merit NASA distribution in English.

SPECIAL PUBLICATIONS: Information derived from or of value to NASA activities. Publications include conference proceedings, monographs, data compilations, handbooks, sourcebooks, and special bibliographies.

TECHNOLOGY UTILIZATION PUBLICATIONS: Information on technology used by NASA that may be of particular interest in commercial and other non-aerospace applications. Publications include Tech Briefs, Technology Utilization Reports and Notes, and Technology Surveys.

Details on the availability of these publications may be obtained from:

SCIENTIFIC AND TECHNICAL INFORMATION DIVISION
NATIONAL AERONAUTICS AND SPACE ADMINISTRATION
Washington, D.C. 20546